Numerical shaper optimization for sputtered optical precision filters

Andreas Pflug*, Michael Siemers, Thomas Melzig, Daniel Rademacher, Tobias Zickenrott, and Michael Vergöhl

Fraunhofer Institute for Surface Engineering and Thin Films IST, Bienroder Weg 54e, 38108 Braunschweig, Germany

**Corresponding author: andreas.pflug@ist.fraunhofer.de*

Received December 10, 2012; accepted December 26, 2012; posted online May 9, 2013

A novel optimization procedure for optical precision sputter coaters with respect to the film homogeneity is demonstrated. For a coater concept based on dual cylindrical sputtering sources and a rotating turn-table as sample-holder, the inherent radial decay of the film thickness must be compensated by shaper elements. For that purpose, a simulation model of the particle flux within such a coater is set up and validated against experimental data. Subsequently, the shaper design is optimized according to the modeled metal flux profile. The resulting film thickness deviations are minimized down to ±0.35%.

OCIS codes: 000.3860, 000.4430, 240.0310, 310.1860.
doi: 10.3788/COL201311.S10204.

Optical precision filters are key components in many different technology areas such as laser technology, medicine and biotechnology, automotive and solar industry as well as high precision instruments. In many cases, very low particle contamination levels together with very good film homogeneity in the range of $\delta d/d \leqslant 0.5\%$ are mandatory. Recently, a novel coater setup called "enhanced optical sputtering system" (EOSS) has been introduced[1], which comprises cylindrical sputtering targets in a sputter-up configuration for minimizing particle contamination of the substrate. This coater features two sputtering compartments with dual-rotatable targets for high- and low-index materials. Substrates mounted on a rotating turn-table are subsequently coated with a thin metallic layer, which gets fully oxidized in a third compartment comprising a plasma oxidation source; this processing scheme aims at precise deposition of absorption-free layers and is further described in Ref. [2].

Due to the circular movement of the turn-table the deposition rate decays reciprocally with radial position, this effect has to be compensated by shaper elements between sputter source and substrate. Since the flux of sputtered particles to the substrate is not homogeneously distributed, it is not sufficient to just linearly increase the shaper orifice as a function of the radius; instead a curved design adapted to the specific material flux profile is required for optimal homogeneity. Thus, the conventional method of designing appropriate shaper elements usually is a time-consuming and critical procedure involving several iterations between sputtering experiments, measuring the film thickness profile and re-constructing the shaper elements by heuristic optimization methods.

This letter presents a numerical optimization method for the shaper elements based on detailed modeling of the particle flux within the coater geometry by direct simulation Monte Carlo (DSMC) method[3]. At Fraunhofer IST, a software tool implementing the DSMC method has been developed, which is capable of handling complex three-dimensional (3D) recipient geometries and makes use of massive-parallelization on high-performance computing resources[4,5]. In a first step, this simulation tool is used to obtain the detailed flux distribution at the substrate surface. Subsequently, the shaper design is obtained by a reverse-optimization procedure with respect to maximal deposition rate homogeneity as a function of the radial position.

For setting up the transport simulation model, a geometric mesh representation of one sputtering compartment of the EOSS coater was created with the open source meshing and postprocessing tool GMSH[6] as shown in Fig. 1. This compartment comprises a dual cylindrical magnetron sputter source together with two Ar inlets and two shapers, which are located just beneath the substrates mounted on the rotary table. The length and diameter of the targets are 660 and 152 mm, respectively; the overall model size is around 0.8 m^3. Two shutters can be optionally placed in front of the substrates in order to enable pre-sputtering; they are included into the transport simulation since their idle position may have some influence on the Ar gas flow.

The Ar gas is fed in via two gas inlet lines located at left and right sides, and a turbo molecular pump is

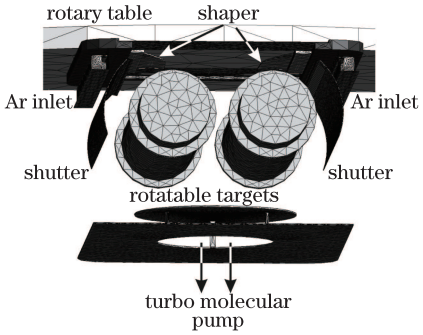

Fig. 1. Meshed geometric model of a sputtering compartment within the EOSS coater.

 © 2013 Chinese Optics Letters

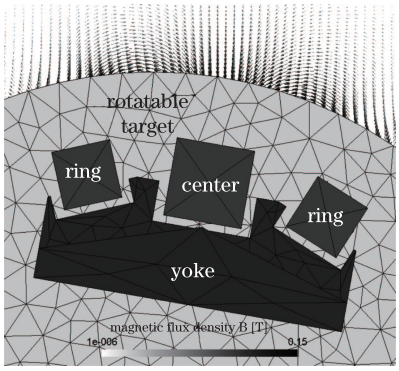

Fig. 2. Magnetic field lines at cylindrical target surface computed by boundary element method.

located at the bottom of the compartment, where it is covered by a protective shielding. The volume on top of the rotary table is pumped by another turbo molecular pump.

In order to determine the location of the race track on the target surface, the magnetic flux density is computed from the magnet assembly via the boundary element method[7] as shown in Fig. 2. The race tracks are approximately located where the magnetic flux density is parallel to the target surface. For a target diameter of 152 mm corresponding to 10 mm of target material, this occurs at two angles of $\pm 14^\circ$ with respect to the symmetry center of the magnetic arrangement. For a reduced target diameter of 138 mm (i.e., 3 mm of material coverage), the race track positions shift slightly towards smaller angles of $\pm 12.5^\circ$, which results from the radial dependency of the magnetic field distribution.

In the DSMC transport simulation, the gas inlets are represented by surfaces where Ar particles are created with a Maxwellian velocity distribution corresponding to a wall temperature of 300 K. For each cylindrical target, the sputtering sources are approximated by two lines located at two angles of $\pm 14^\circ$ from the center of the magnet systems, and both magnet systems are tilted by 10° towards each other. At the sputtering sources, Nb atoms are inserted into the simulation system with a Thompson energy distribution and a $\cos^n(\theta)$ like angular distribution, i.e.,

$$f(E,\theta) = \cos^n(\theta)\frac{E}{(E+U_0)^3}, \tag{1}$$

where E is the energy, U_0 is the binding energy, θ is the polar emission angle, and n is a material dependent index. For Nb, a binding energy of $U_0 = 7.4$ eV and an index of $n = 1$ were chosen according to published data[8]. A total Ar flux of 2×50 sccm was applied, for the total sputtering flux, and an equivalent of 20 sccm per sputter target was assumed. The turbo pump at the bottom was represented by an effective circular pumping surface with 14% absorption probability for Ar. With a diameter of 214 mm and a mean thermal velocity of Ar at 300 K of 398.5 m/s, this yields an effective pumping speed of 0.5 m^3/s.

The scattering behavior of the Ar atoms can be expressed by energy-dependent collision cross sections. We apply the variable softsphere model[3,9], where the expression for the energy-dependent cross section $\sigma(E)$ is

$$\sigma(E) = \pi d_{\mathrm{ref}}^2 \frac{(kT/qE)^{\omega_{\mathrm{ref}}-0.5}}{\Gamma(2.5-\omega_{\mathrm{ref}})}. \tag{2}$$

Parameters for Ar were the atomic reference diameter $d_{\mathrm{ref}} = 4.11\times 10^{-10}$ m and the viscosity index $\omega_{\mathrm{ref}} = 0.81$. For the scattering of the Nb metal atoms within the gas phase, an approach[10] based on the Born-Meyer approximation for the interatomic potentials[11] was implemented.

The given process parameters yield an equilibrium pressure of Ar in the range of 0.35 Pa, where the mean free path of Ar is in the range of 2 cm. A cell resolution of the DSMC computation of approximately 8 mm was chosen. With the geometric dimensions given above the 3D simulation model consists of about 1.536 million DSMC cells in total. The selected time step was 1 μs, while the simulated total physical time interval was in the range of 1.5–2 s corresponding to 1.5–2.0 million DSMC time cycles. Typical computation demands were about 24 CPU cores for 48 h on an AMD "Magny-Cours" 6 172 based Linux cluster installed at Fraunhofer IST.

With the metallic sticking coefficients of the inner chamber walls assumed to be 100%, the distribution of the deposited metal can be extracted after accumulation during several DSMC simulation cycles. For the deposition profile shown in Fig. 3, time averaging of the DSMC simulation is performed between 1.4 and 1.6 s, which corresponds to 200 000 DSMC cycles. The area of the substrate which is reachable from the sputter sources through the shielding orifices, is highlighted in this picture. The inhomogeneous metal flux profile arising from the position and shape of the race tracks of the targets, is clearly visible.

In order to obtain the radial deposition profile from these data, the deposition flux profile on the substrate plane has to be integrated along circular paths concentric with the rotary table. At each point of the circular path, the effective metal flux has to be extracted from the discretized DSMC data by bilinear interpolation.

The result of the interpolation and integration procedure can be seen in Fig. 4, where the simulated radial deposition profiles from different setups are compared with film thickness measurements on test samples by spectroscopic ellipsometry. The first scenario shown here corresponds to the case, where no shapers are installed at all. As a result, the film thickness decreases reciprocally with radius. This behavior is well

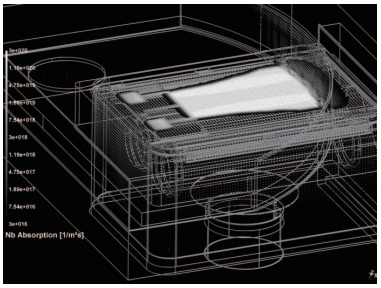

Fig. 3. Simulated Nb metal deposition flux onto the inner surfaces of the EOSS coater. The highlighted area corresponds to the substrate surface which can be reached from the sputter targets through the shaper orifice.

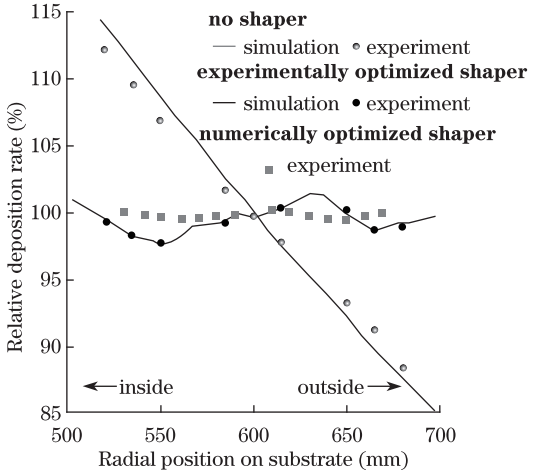

Fig. 4. Radial deposition profiles as extracted from the DSMC simulation runs and as measured by spectroscopic ellipsometry from test samples.

reproduced in the simulation model as well as by the experiments. The second scenario shown in Fig. 4 corresponds to a shaper design, which has been empirically obtained. In this procedure, a first shaper version is constructed with a reasonable starting design, and film thickness profiles are determined by sputtering experiments and spectroscopic ellipsometric evaluation of the test samples. Afterwards the shaper design is refined according to the measured film thickness deviations. The result shown in the second curve of Fig. 4 corresponds to the second empirical iteration of the shaper design, and the overall deposition homogeneity is in the range of $\delta d/d = 2\%$. There is a remarkably good agreement between measurement and simulation.

For the numerical shaper optimization, in a first step the metal flux profile to the substrate is taken from a DSMC simulation run with no shaper at all. In the second step, the radial profile is computed by circular integration over the deposition flux profile as described above. Additionally, a parameterized function of the shaper boundary is introduced. In order to be compatible with the CNC cutting machine used for fabricating the shaper designs, the boundary curve consists of several circular segments, where the coordinates and radii can be treated as free parameters. This parameterized description of the shaper boundary is introduced into the circular integration procedure. By bilinear interpolation and cutting off the region beneath the shaper surface, a deposition profile results, where the effect of the shaper has been taken into account. This approach is possible since the shaper is located only about 2 mm beneath the substrate plane; thus it is reasonable to neglect further gas phase scattering of the metal flux between shaper and substrate. The radial deposition profile function is subsequently put into a least-squares fitting algorithm based on the Simplex method for function minimization[12]. The function $f_{\min}$ to be minimized is just the accumulated square deviation of the actual deposition rate $f(R)$ from a fixed absolute value R_0, which can be also varied within a certain range:

$$f_{\min} = \sum (f(R) - R_0)^2. \quad (3)$$

The shaper boundary used within the minimization procedure consists of two linear segments with fixed coordinates and four circular segments, whereof the radii and coordinates of the junction points can be varied. In total, 12 parameters are varied within the simplex fitting algorithm. The resulting shaper boundary is manufactured by the CNC cutting machine, and the resulting experimental film thickness profile shows significantly reduced film thickness deviations in the order of $\delta d/d = 0.35\%$ (see the third curve in Fig. 4).

It has to be mentioned that the shaper optimization procedure shown here relies on the assumption that the cylindrical targets have a homogeneous sputter erosion profile in longitudinal direction at least within the straight section facing the substrate. During the experiments, this was not always the case. In case of ceramic targets, e.g., certain inhomogeneities in the bonding of the target material may cause visible deviations. For reactive sputtering processes with oxygen as reactive gas, a non-symmetric gettering behavior of the surrounding surfaces of the chamber may cause a "tilted" distribution of the target erosion, which would have a strong effect on the sputter rate distribution. Thus, the very first step of the optimization procedure must be always to ensure a symmetric operation state of the targets, which may involve some additional process control equipment such as manifold gas inlets and separated partial pressure measurement gauges.

In conclusion, the DSMC simulation method is proven to describe the flux of gaseous and metal particles within a sputter process in an accurate way. The DSMC method is applied to the geometry of the EOSS sputter coater in order to compute the metal flux profile to the substrate and take into account the effect of different shaper designs on the resulting film thickness profile. Combining this approach with a numerical fitting method allows for refining the boundary of the shaper in an automated way aiming for minimized film thickness deviations. This shaper optimization method is based on the assumption that the sputter erosion along the target axis is evenly distributed, which may require applying appropriate means of $in-situ$ process control. In case of the EOSS system, it is possible to reduce the film thickness deviations to $\delta d/d \leqslant 0.35\%$ by means of the numerical optimization procedure, which is a significant improvement compared with previous empirically obtained shaper designs. Besides optimization, the DSMC simulation method can be used to study the influence of various long-term drifts such as erosion of the target or mechanical tolerances on the deposition profile. As a result, the steps required for the development of stable and homogeneous deposition processes can be prioritized in a systematic way.

The development of the DSMC/PIC-MC simulation tool was partly supported by the VolkswagenStiftung within the joint project "Cosmos" (I83/234), which is greatly acknowledged by the authors.

References

1. D. Rademacher, G. Bräuer, M. Vergöhl, B. Fritz, and T. Zickenrott, Proc. SPIE **8168,** 81680O (2011).
2. J. P. Lehan, R. B. Sargent, and R. E. Klinger, J. Vac. Sci. Technol. A **10,** 3401 (1992).

3. G. A. Bird, *Molecular Gas Dynamics and the Direct Simulation of Gas Flows* (*Oxford Engineering Science Series*) (Clarendon Press, Oxford, 1994).
4. A. Pflug, M. Siemers, and B. Szyszka, Lect. Notes Comput. Sci. **4192,** 383 (2006).
5. C. Schwanke, A. Pflug, M. Siemers, and B. Szyszka, Lect. Notes Comput. Sci. **7133,** 213 (2012).
6. C. Geuzaine and J.-F. Remacle, Int. J. Numer. Meth. Eng. **79,** 1309 (2009).
7. C. A. Brebbia and R. Magureanu, Eng. Anal. **4,** 178 (1987).
8. Y. Yamamura, T. Takiguche, and M. Ishida, Radiat. Eff. Defect. Solid. **118,** 237 (1991).
9. K. Koura and H. Matsumoto, Phys. Fluids A **4,** 1083 (1992).
10. S. S. Nathan, G. M. Rao, and S. Mohan, J. Appl. Phys. **84,** 564 (1998).
11. A. A. Abrahamson, Phys. Rev. **178,** 76 (1969).
12. J. A. Nelder and R. Mead, Comput. J. **7,** 308 (1965).